P1.102 DATA IMPACT EXPERIMENTS USING IASI OBSERVATIONS DURING THE LIFE CYCLE OF HURRICANES GUSTAV, HANNA AND IKE (2008)

Doris Anwender *, Nadia Fourrie, Florence Rabier, Philippe Arbogast
Karlsruher Institut für Technologie

1. INTRODUCTION

The numerical forecast of the extratropical transition (ET) of a tropical cyclone (TC) is difficult because of the relatively small scales of the TC and the associated convection. This can result in large errors of the first guess. Furthermore, the ET system may carry a huge amount of the moisture of the ex-TC along, which can lead to strong precipitation and flooding events over the adjacent continent. The water vapor transport from the decaying TC into the midlatitudes is an important issue for the correct prediction of an ET. Hence, for ET cases a good coverage of observations which are introduced in the data assimilation systems is important.
The in-situ data distribution is very heterogeneous and in some regions very sparse, i. e. over the oceans and especially over the poles. Vast improvements in numerical forecasts have been achieved by the use of the hyperspectral infrared instruments AIRS (advanced infrared sounder) and IASI (infrared atmospheric sounding interferometer). Andersson et al. (2007) studied the impact of humidity data on analysis and forecast. They found a significant impact of microwave and infrared sounders and also of surface stations which extended into the medium range.
Our study is dedicated to the impact that additional observations in general and additional observations taken by the IASI instrument have on the prediction of ET cases. A period in September 2008 was chosen in which three tropical cyclones underwent ET over the Atlantic or the United States which were related to distinct atmospheric developments over Europe and the Mediterranean Sea.
In one of the experiments the observation density in the data assimilation system during the ET periods is tested. Liu and Rabier (2003) have shown in their study with simulated observations that in the case of uncorrelated observation errors enhancing the density can improve the analysis and the forecast in general. However, if the observation errors are correlated and the correlation length exceeds a certain threshold enhanced observation density can degrade analysis and forecast. Another experiment is designed to investigate the influence of IASI data on the analysis and forecast. In a further experiment the influence of additional IASI humidity observations, which improve the representation of the important moisture processes during an ET, is investigated.

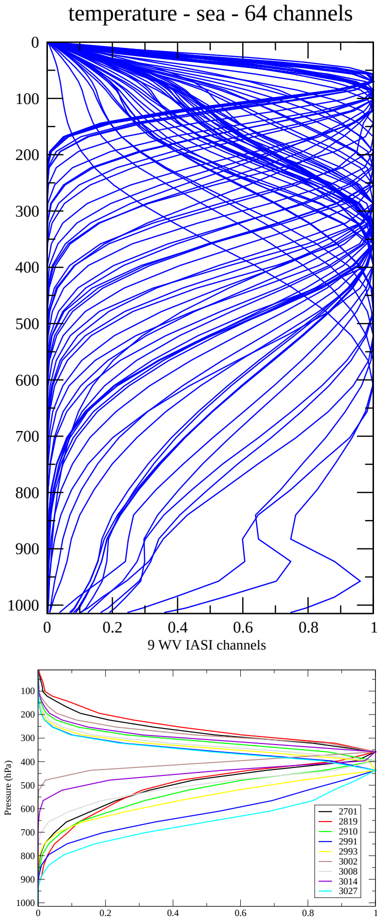

FIG. 1: Weighting functions of assimilated channels for IASI (top). Water vapor channels added for the second experiments (bottom).

2. THE EXPERIMENTS

The global spectral model ARPEGE with spectral triangular truncation T538 of Meteo France is used for the data impact experiments. The model has a stretched grid with a stretching factor of 2.4, i. e. the resolution above the area of interest is 2.4 times higher (horizontal about 15 km) and that over the antipode is 2.4 times lower (horizontal at about 90 km) than the mean. The region with the maximum resolution can be moved over the area of interest but is in general centered on Europe. The vertical resolution of ARPEGE is 60 levels in hybrid coordinates.

*Corresponding author address: Doris Anwender, Institut für Meteorologie und Klimaforschung, Wolfgang-Gaede-Str. 1, Karlsruhe; e-mail:doris.anwender@kit.edu

To calculate the analysis with ARPEGE a four-dimensional variational (4D-Var) data assimilation system with an assimilation window of 6 hours is used. The analysis is produced four times daily from the background which is a 6 hour forecast from the previous analysis, and the data present from 3 hours before and 3 hours after the analysis time.

Four experiments are performed over a 20 day period from 1 to 20 September 2008. In the high density experiment (DENS) the density of all the assimilated observations is 3.5 times higher then in the control forecast over the whole globe. In the ARPEGE model the globe is divided in boxes with 250 km side length. One data point is chosen from each box. To enhance the density each box is replaced by four boxes with side lengths 125 km.

The instrument IASI measures radiances in the thermal infrared region from 645 - 2760 cm^{-1} with a spectral sampling of $0.25cm^{-1}$. Currently, 64 selected IASI channels are assimilated in the operational suite only over sea and only clear-sky. Each channel has an appropriate weighting function which determines from which level the measured radiance originates. In Figure 1 (top) the 64 IASI channels are shown. For the second experiment (NOIASI) all the IASI observations are switched off.

Additional humidity observations for the third experiment (IASIWV) will be taken by selecting nine IASI water vapor channels which will be assimilated additionally (Fig. 1, bottom). They are mainly sensitive to the upper troposphere as they obviously peak between 350 and 450 hPa.

The impact of the high density is determined by a comparison of the analysis and forecasts to the fourth, the control experiment (CTRL), which uses the operational observation density. The impact of the experiment without IASI data and of the humidity sensitive radiances is evaluated comparing the results to DENS.

3. RESULTS

3.1 *Global Scores*

The global forecast error is calculated between one specific experiment and the independent ECMWF analysis. The global impact is the difference between this forecast error and the forecast error between the respective control experiment and the ECMWF analysis.

The impact of DENS in comparison with CTRL is positive for all the variables (e. g. Fig. 2) over the northern and southern hemisphere in the troposphere and in the tropics. The positive impact is significant for about 60 hours in the northern hemisphere and for 84 to 96 hours in the southern hemisphere and the tropics for all variables.

The impact of omitting all the IASI data is negative on the northern and southern hemisphere (e. g. Fig. 3). In the southern hemisphere the negative impact is significant for the temperature for up to 60 hours in the mid troposphere and for the humidity for 84 to 96 hours in the low tropopause. In the northern hemisphere the impact is significant for about 24 hours mostly in the mid- and upper troposphere. In the tropics, however, the impact of omitting IASI data is positive. The significance for the geopotential is particularly strong for the mid- and upper troposphere for up to 48 hours. For the other variables the layers of positive significance are thinner and mainly in the lower tropopause for about 24 hours.

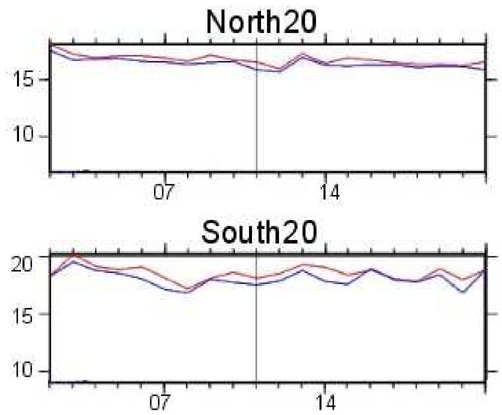

FIG. 2: Errors for 20 24-hour forecasts with respect to the EC analysis from 2 - 21 September 2008. DENS (blue) versus CTRL (red) for the northern hemisphere down to 20° N (top) and the southern hemisphere up to 20° S. Errors of the 500 hPa relative humidity (%).

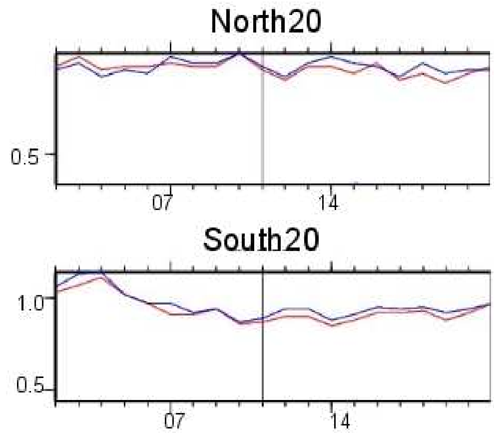

FIG. 3: Errors for 20 24-hour forecasts with respect to the EC analysis from 2 - 21 September 2008. NOIASI (blue) versus DENS (red) for the northern hemisphere down to 20° N (top) and the southern hemisphere up to 20° S. Errors of the 500 hPa temperature (K).

3.2 *Impact Of Water Vapor Channels Over Atlantic / Europe*

The variables important for the description of the transformation of a TC, for which the global impact in the previous section was calculated individually, are combined into the total energy for the investigation of the impact of the water vapor channels over the Atlantic and Europe. The absolute error is calculated for the Atlantic domain, i. e. 60° - 20° W and 25° - 65° N, and for the European domain, i. e. 20° W - 20° E and 25° - 65° N, separately, and is determined analogous to the previous section using the total energy as variable.

The impact of the additional IASI channels over the At-

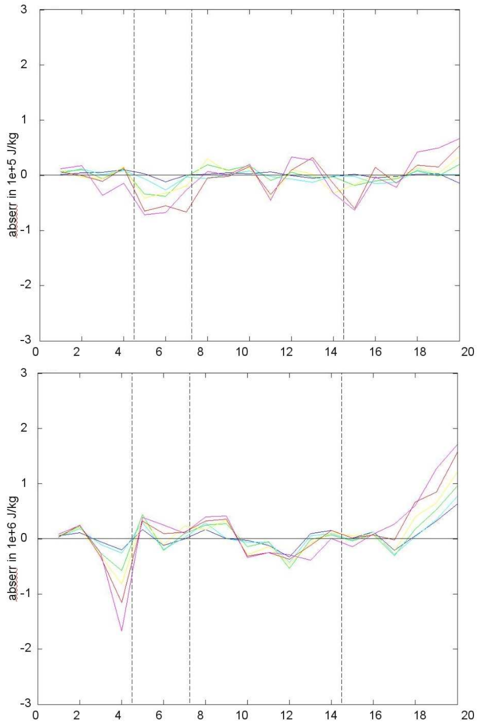

FIG. 4: Top: Atlantic domain. Absolute error $E(x)$ of total energy between IASIWV and DENS for 1 to 20 September for 00 - 30 hours (Jkg^{-1} * 1e+5) (top) and 72 - 102 hours (Jkg^{-1} * 1e+6) (bottom) forecast time. Rainbow colors from the respective earliest (blue) to the respective latest (magenta) forecast time. ET times marked by a dashed line.

lantic on the short forecast range is mostly positive, i. e. the values in the differences of absolute error between IASIWV and DENS are negative as they show smaller errors in IASIWV (Figs. 4, top). Negative peaks are seen at 5 - 7 and 15 September, i. e. around or shortly after the ETs. They are associated with a lower absolute error of the total energy in IASIWV in the region of the ET event or downstream. For the long forecast ranges one clear peak of error reduction due to IASIWV is seen at the 4 September (Fig. 4, bottom). The error reduction over the Atlantic for the forecast from 4 September is strongly related to the ET of Hanna. Over the Atlantic domain an error increase in IASIWV in comparison to DENS is seen in the mid and long range from about 18 September. The error, which is due to differences in the midlatitude jet and not due to an ET event itself, propagates into a cut-off low which was created under the influence of Ike.

Over Europe most of the short range forecast error differences (Fig. 5, top) are slightly positive in contrast to that over the Atlantic domain (Fig. 4, top). However, two distinct negative peaks can be seen on 6 and on 17 September, i. e. 36 h after Gustav's and 60 hours after Ike's ET.

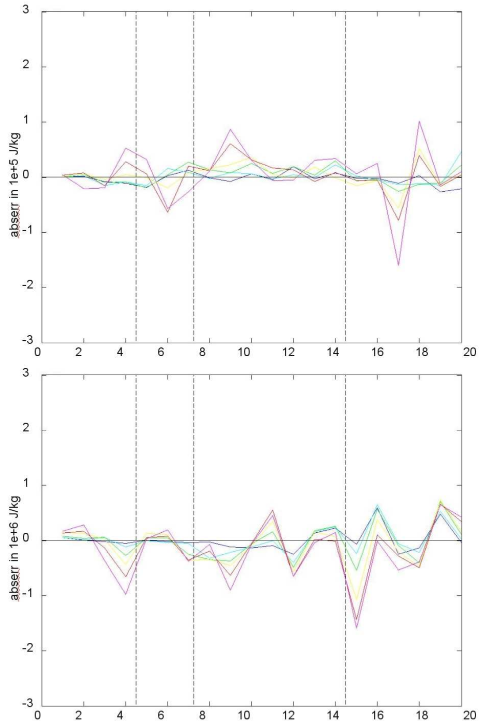

FIG. 5: As Fig. 4 for the European domain.

The negative peak on 6 September over Europe is not associated with an ET event as a blocking ridge is inhibiting any downstream propagation from the deep pressure system east of Greenland. The decrease of error on 17 September for the short range for the 30 hour forecast (Fig. 5, top) is associated with a cut-off low developing downstream of a strong ridge carrying along Ike.

The values in the longer range forecasts are mostly negative (Fig. 5, bottom). Peaks are seen on 4, 9, 12 and 15 September. The error reduction seen for 4 September is downstream of a deep pressure system which may contain the remnants of Gustav. The negative peak on 9 September is not obviously associated to an ET event. On 12 September and 15 September the negative values are associated with the trough forming downstream of the ridge carrying along Ike and the development of a cut-off low from this trough.

3.3 *A Case Study*

One of the dates with strong negative peaks in the absolute error between IASIWV and DENS over the European domain, the 15 September, was chosen for a case study to get more detailed insight into the relation of the error reduction in IASIWV to the ET events and to investigate the downstream propagation of the error reduction.

On 15 September 00 UTC, i. e. 12 hours after Ike completed ET, the ex-TC starts to merge with an extratropical system (Fig. 8). The resulting deep pressure system is located over the Great Lakes stretching towards Newfoundland. The jet stream at 200 hPa develops a distinct ridge.

The analysis error variance in observations space,

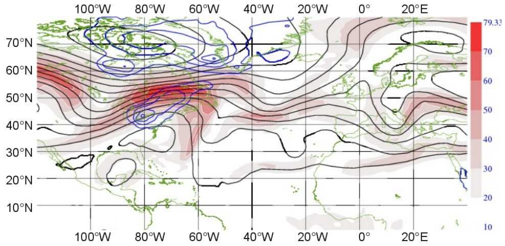

FIG. 6: ECMWF analysis for 15 September 00 UTC, i. e. during the life-cycle of Ike. Horizontal wind at 200 hPa (ms^{-1}, shaded), 200 hPa geopotential (gpdam, black contours), surface pressure less than 1005 hPa (hPa, red contours).

which can be determined by the quantity (analysis - forecast)*(observation - analysis) (detailed description in Desroziers et al. (2005)), is shown for the ARPEGE analysis on 15 September 00 UTC (Fig. 7). In regions in which the values are orange or red, the quality of the analysis is substantially worse than that produced by the model on average. The values are blue if the quality of the analysis is considerably better than that produced by the model on average. Enhanced values in the analysis error variance give information in which regions the assimilation of the observations did not yield much benefit.

On average the analysis error variance in NOIASI is largest in scale and amplitude (Fig. 7, top). They are seen over large areas in the mid-Atlantic, in the Caribbean region and east of Newfoundland. In the ECMWF analysis it was seen that the region over Newfoundland is associated with ex-Ike (Fig. 6). High analysis error variance is found in the region of the ridge forming directly north of Ike. In DENS (Fig. 7, middle) the analysis error variance is much more localized. The error values in the region east of Newfoundland are higher than in NOIASI but the scales are much smaller in DENS. Enhanced analysis error variance in DENS is found in the vicinity of the jet streak. IASIWV shows the smallest analysis error variance (Fig. 7, bottom). The error is as localized as for DENS but the enhanced values close to the jet streak are smaller in IASIWV.

Comparing the differences of the total energy between IASIWV and DENS (Fig. 8) we note a downstream propagation of the error reduction due to the additional water vapor channels from the deep pressure system associated with ex-Ike. On 16 September 12 UTC a huge ridge has formed at 200 hPa extending from the eastern United States to Iceland (not shown). The deep pressure system resulting from ex-Ike reintensifies and propagates quickly along the jet stream associated with this ridge. On 18 September, i. e. for a 72 hour forecast, the eastward tilting of the crest of the ridge cause the formation of a cut-off low west of Portugal (Fig. 8, top). Error reductions in IASIWV are seen in ex-Ike, which is located over Ice-

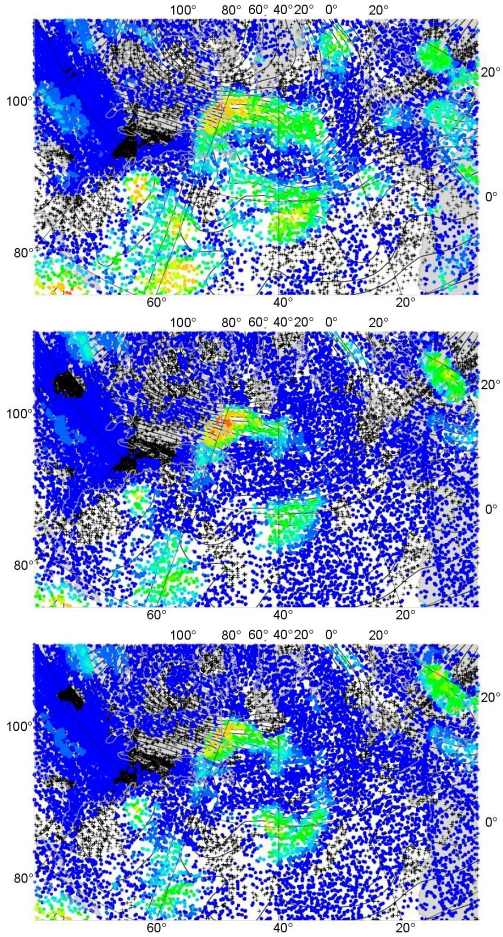

FIG. 7: Error variance of the analysis in observation space for noiasi (top), dens (middle) and iasiwv (bottom) at 15 September 2008 00 UTC. Blue colors denote small errors and red denote big errors with respect to a 3 monthly average error variance. Pluses denote regions where the model and the observations are very close. 200 hPa geopotential in ECMWF analysis.

land, close to the crest of the ridge located over Ireland, and on the western and eastern flanks of the cut-off low. Twelve hours later the fields of error reduction increase in scale and amplitude and propagate from the eastern flank of the cut-off downstream into the adjacent ridge (Fig. 8, middle). On 19 September 00 UTC large regions of strong error reduction due to the water vapor channels are seen over Europe (Fig. 8, bottom). They shift to the east with the crest of the ridge and broaden and intensify further in the cut-off low and in the ridge directly downstream.

Investigations of the potential temperature fields (not shown) showed that the error reductions are associated with a differing representation of the shape of the PV streamer west of Portugal in IASIWV and DENS. In DENS the upper level trough associated with the cut-off low is deeper and the temperatures in the ridge over North Africa are higher than in IASIWV.

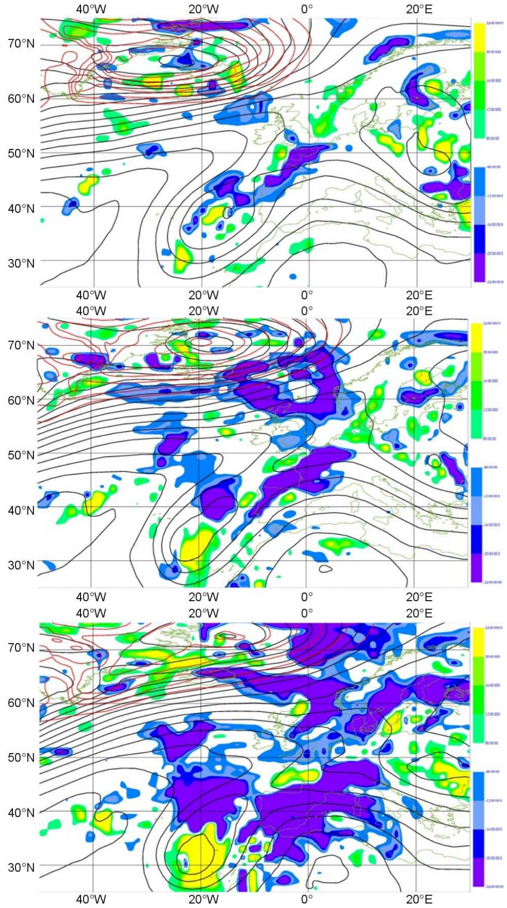

FIG. 8: Forecasts of difference of total energy between IASIWV and DENS (shaded, ci: 8e+5*Jkg^{-1}), 200 hPa geopotential (black contours, ci: 5 gpdam), mean sea level pressure $\leq$ 1005 hPa (red contours, ci: 5 hPa) initialized on 15 September 00 UTC for 72 hours (top), 84 hours (middle) and 96 hours (bottom) forecast time. Purple to blue colors: error reduction in IASIWV, green to yellow colors: error increase in IASIWV.

We suppose that the better representation of the ridge associated with Ike's ET due to the additional water vapor channels (Fig. 7, bottom) plays an important role in the improvement of the forecast of the propagation and shape of the ridge, of the cut-off low downstream and of the ridge further downstream.

4. CONCLUSION AND OUTLOOK

Our investigations showed a strong importance of the IASI observations for the numerical forecast of ARPEGE. The impact of the additional water vapor channels was less obvious in the global scores but hints are found that errors in the representation of the synoptic fields during the three investigated ETs have been better corrected due to the water vapor channels.

A further investigation of the improvement of the forecast in the individual variables which contribute to the total energy are desirable. The dynamics of downstream propagation in the individual fields and their connection to each other need to be further explored to understand the propagation of error reduction.

We plan to extend this study to extratropical storms. This could illustrate the role that the water vapor plays in the extratropics and give hints on other important variables. Furthermore, it would be desirable to calculate the sensitive regions for the investigated cases and connect them with the locations and times of error reductions.

Morss and Emanuel (2002) showed that the risk of degrading the forecast even with perfect observational data and a perfect forecast model is inherent in statistical data assimilation like 4D-Var. They suggest that assimilating added data is better interpreted as probabilistic than deterministic. For this purpose, experiments with an ensemble of slightly differing analysis might yield more consistency in the impact of additional data.

REFERENCES

Andersson, E., E. Holm, P. Bauer, A. Beljaars, G. A. Kelly, A. P. McNally, A. J. Simmons, J.-N. Thepaut, and A. M. Tompkins, 2007: Analysis and forecast impact of the main humidity observing systems. *Quart. J. R. Meteorol. Soc.*, **133**, 1473–1485.

Desroziers, G., L. Berre, B. Chapnik, and . P. Poli, 2005: Diagnosis of observation, background, and analysis error statistics in observation space. *Quart. J. Roy. Meteor. Soc.*, **131**, 3385–3396.

Liu, Z.-Q. and F. Rabier, 2003: The potential of high-density observations for numerical weather prediction: A study with simulated observations. *Quart. J. R. Meteorol. Soc.*, **129**, 3013–3035.

Morss, R. E. and K. E. Emanuel, 2002: Influence of added observations on analysis and forecast errors: Results from idealized systems. *Quart. J. R. Meteorol. Soc.*, **128**, 285321.